Revista Mexicana de Astronomía y Astrofísica, **00**, **??**–10 (2000)

DETAILED ATMOSPHERIC ABUNDANCE ANALYSIS OF THE OPTICAL COUNTERPART OF THE IR SOURCE IRAS 16559-2957

R. E. Molina,[1] and A. Arellano Ferro[2]

Received January 16, 2013; accepted January 16, 2013

RESUMEN

Hemos emprendido un análisis detallado de las abundancias químicas de la contraparte óptica de la fuente infrarroja IRAS 16559-2957 con el fin de confirmar su posible naturaleza de estrella post-AGB. El análisis de un gran número de elementos, incluidos CNO y $^{12}C/^{13}C$, muestra que este objeto ha experimentado el primer dragado y parece estar aún en fase de RGB.

ABSTRACT

We have undertaken a detailed abundance analysis of the optical counterpart of the IR source IRAS16559-2957 with the aim of confirming its possible post-AGB nature. The star shows solar metallicity and our investigation of a large number of elements including CNO and $^{12}C/^{13}C$ suggests that this object has experienced the first dredge-up and it is likely still at RGB stage.

Key Words: **STARS: ABUNDANCES - STARS: EVOLUTION - STARS: PAGB - RGB PHASE**

1. INTRODUCTION

Post-AGB stars (PAGB's) are at a very advanced stage of evolution. They show peculiarities in the observed elements in their atmospheres (e.g. CNO and s-process elements abundances) which are connected with the dredge-up episodes that occur as the star evolves up on the AGB. PAGB's also have high mass loss ($\geq 10^{-6}$ $M_\odot$/yr) which obscures the central star and produces emission in the IR and OH masers (Zijlstra et al. 1989). Consequently, the IRAS color-color diagram ([25]-[60],[12]-[25]) and its IRAS variability has been widely used in the identification of PAGB and proto Planetary Nebulae (PPN) candidates (van der Veen & Habing 1988; García-Lario et al. 1997; Suárez et al. 2006; Szczerba et al. 2012).

The identification of optical counterparts of IR and OH masers and IRAS sources is of fundamental importance since it is in the optical spectrum that the abundance anomalies of structural and evolutionary relevance can be detected and studied, such as CNO abundances and those of s-process elements (e.g. La, Ba, Nd, Sr, Y, Zr).

The IRAS 16559-2957 source has been included in several studies aimed to identify and evaluate the evolutionary status of large lists of PAGB and PPN candidates. In the finding chart provided by Hu et al. (1993) (their object 34) there is only one bright star within the IRAS beam. According to Hu et al. it is a F5I star of $V \sim 13$ with Hα filled in. The presence of a circumstellar envelope around a central star was confirmed by the detection of strong OH maser at 1612 and 1665 MHz (Hu et al. 1993). The radial velocity of OH maser profile varies between 57–70 km s^{-1} (te Lintel Hekkert et al. 1991).

The source was included in the sample of PAGB and PN candidates studied by Suárez et al. (2006) who find no optical counterpart. However, Ramos-Larios et al. (2009), in their search of heavily obscured PAGB and PN stars found a near-IR counterpart in the 2MASS Point Source Catalogue and an optical couterpart in the Digital Sky Survey, which corresponds to a $V \sim 13.2$ star (see their finding chart on Fig. 3), in agreement with Hu et al. (1993). Then the star has been "bona fide" catalogued as a PAGB (e.g. Szczerba et al. 2007; SIMBAD [3]data base).

With the aim of confirming the PAGB nature of the optical counterpart we have studied a high resolution optical spectrum of the $V \sim 13.2$ star at RA $\alpha = 16^h59^m08.2^s$, Dec. $\delta = -30°01'40.3''$. In

[1]Laboratorio de Investigación en Física Aplicada y Computacional, Universidad Nacional Experimental del Táchira, Venezuela.

[2]Instituto de Astronomía, Universidad Nacional Autónoma de México, México.

[3]http://simbad.u-strasbg.fr/simbad/sim-fid

TABLE 1

ATMOSPHERIC PARAMETERS OF IRAS 16559-2957.

$T_{\rm eff,sp}$ (K)	log g_{sp}	$\xi_{t,sp}$ (km s^{-1})
4250	1.5	1.43

this paper, we present a photospheric detailed chemical abundances analysis of this optical source and we shall refer to the object as IRAS 16559-2957.

The paper is organized as follows: in § 2 the observations and reductions are described, in § 3 we discuss the adopted atmospheric parameters and the reddening, in § 4 we employed the equivalent widths and spectral synthesis approaches to derived the photospheric chemical abundances, in § 5 we discuss our results, and in § 6 we summarize our conclusions.

2. OBSERVATIONS AND REDUCTIONS

The spectrum of IRAS 16559-2957 (V=13.2) was obtained on February 27, 2008 with the 2D Coudé echelle spectrograph (Tull et al. 1995) on the 2.7m telescope at the McDonald Observatory giving $\sim$ 40,000 resolution and a wavelength coverage from 3900 to 10000 Å . The spectrum was reduced using the IRAF astronomical routines. The equivalent widths (EW's) were measured using the SPLOT task and their accuracy is generally better than 10% for spectra with S/N ratio larger than 50. We generally restricted ourselves to unblended weak features and avoided using lines stronger than 200 mÅ.

We measure the heliocentric radial velocity using the Doppler shift of 40 clean unblended absorption lines that cover a wide spectral range. We derive a heliocentric radial velocity of -2.3 ± 0.5 km s^{-1} ($V_{\rm LSR} = +7.1$ km s^{-1}).

3. ATMOSPHERIC PARAMETERS

Before we derive the elemental abundances it is necessary to estimate the fundamental atmospheric parameters; effective temperature, surface gravity and microturbulence velocity. We have approached the task as discussed in the following subsections.

3.1. *Spectroscopy*

An independent estimation of $T_{\rm eff}$, log g and the microturbulence velocity ξ_t can be obtained from the behavior of the lines of a well represented element (e.g. Fe), and the `MOOG` code (2009 version) by C. Sneden (1973), which is based on local thermodynamical equilibrium (LTE) calculations. We employed the atmospheric model collection of Castelli & Kurucz (2003).

We have therefore followed the standard procedure for temperature and gravity determinations. For temperature, it is required that the Fe I abundances are independent of the low excitation potential of the lines. The gravity can be derived by requiring that the Fe I and Fe II lines yield the same abundance. This procedure led to values $T_{\rm eff}$ = 4250 ± 200K and log g=1.5±0.25. This effective temperature does not correspond to a star of spectral type F5I but it is more typical of an early K-type star.

The microturbence is estimated by requiring that the derived abundances are independent of the line strengths for a given specie. Generally, lines of Fe II are preferred. It is known that Fe II lines are not seriously affected by departure from LTE (Schiller & Przybilla 2008). On the contrary Fe I lines are affected by NLTE effects (Boyarchuck et al. 1985; Thévenin & Idiart 1999). For cool stars however not many Fe II lines are available. The microturbulence velocity, is therefore determined using the error diagram for Fe I or Fe II (depending on the number of measured lines). For a given model, we compute the dispersion in the Fe abundances over a range in the microturbulence velocity using the method of Sahin & Lambert (2009). Fig. 1 shows the standard deviation σ_x as a function of microturbulence velocity ξ_t for Fe I and Fe II lines. From the minimum error we estimate ξ_t =1.43 km s^{-1}.

3.2. *Determination of E(B-V)*

The initial effective temperature of IRAS 16559-2957 could also be estimated from JHK photometry available in the work of Cutri et al. (2003) and the $T_{\rm eff}$ calibrations of Alonso et al. (1999) from the $J-H$ and $V-K$ colours. However, a previous knowledge of the reddening would be necessary. Instead we have used the calibrations to estimate the total extinction. The insterstellar extinction maps of Schlegel et al. (1998) lead to a value $E(B-V) = 0.38$, and after applying the correction recommended by Bonifacio et al. (2000) for exceses larger than 0.15, we find $E(B-V) = 0.28$. Since the star is affected by circumstellar material responsible of the OH masser and IR excess, we have increased the value of $E(B-V)$ until the calibrations of Alonso et al. (1999) produce a value of $T_{\rm eff}$ $\sim$4250K, esti-

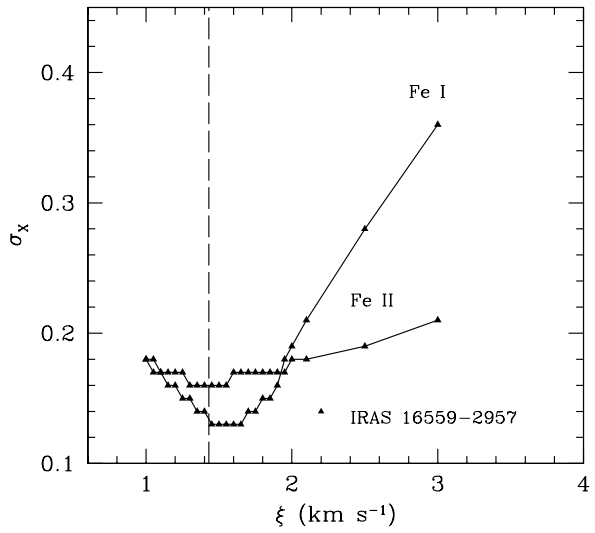

Fig. 1. The standard deviation of Fe I and Fe II abundances as a function of microturbulence velocity for IRAS 16559-2957. The dotted vertical line corresponds to the value of the adopted microturbulence velocity.

mated spectroscopically. The total, interstellar plus circumstellar, reddening is $E(B-V) = 0.81$, leaving $E(B-V) = 0.53$ as our estimation of the circumstellar contribution.

The basic photometric and spectroscopic atmospheric parameters are resumed in Table 1. The adopted values for the atmospheric parameters are indicated by the lower subscript "sp".

The models of Castelli & Kurucz (2003) are calculated in steps of ± 250 K, ±0.5 and ±0.25 km s^{-1} in $T_{\rm eff}$, log g and ξ_t respectively. We have used however a set of interpolated models in steps of ±100 K, ±0.25 and ±0.20 km s^{-1}. The sensitivity of the derived abundances to the uncertainties of atmospheric parameters are given in Table 2 were we present changes in abundances caused by varying atmospheric parameter by the above amounts with respect to the chosen model.

4. ATMOSPHERIC ABUNDANCES

4.1. *Equivalent Width Analysis*

To calculate the atmospheric abundances we have used the 2009 version of the code `MOOG` (Sneden 1973) which performs LTE line analysis. We use the grid ATLAS9 of plane-parallel model atmosphere computed by Castelli & Kurucz (2003). Chemical abundances of well represented elements were determined through the analysis of equivalent widths using the *abfind* driver in MOOG code.

The oscillator strength or gf value is an important atomic parameter that affects the abundance calculations. The gf values can be obtained from numerous sources, and the uncertainties vary from element to element. For example, experimental values for Fe I and Fe II of high accuracy, between 5 to 10%, are available for a large fraction of lines. For other Fe-peak elements, errors in their gf values may range between 10 to 25%. For neutron-capture elements the accuracy of recent estimates are in 10% to 25% range. An extensive list of gf values for all important elements can be found in Sumangala Rao, Giridhar & Lambert (2012).

The sensitivity of the derived abundances to the uncertainties in the model atmosphere parameters $T_{\rm eff}$, log g and ξ_t are summarized in Table 2. We present abundance variations caused by changes in atmospheric parameters of 100 K, 0.25 dex and 0.2 km s^{-1} respectively, relative to the selected model. We have evaluated the total error in the abundance of a given element, by taking the square root of the summation of the squares of the errors associated to $T_{\rm eff}$, log g and ξ_t. From the uncertainties listed in Table 2, we find the total absolute uncertainty to be ranging from 0.05 for C to 0.29 for Fe II.

4.2. *Spectrum Synthesis Analysis*

In this section we discuss the determination of abundances of light elements CNO. Some lines that are blended or affected by the hyper-fine structure were analyzed by spectral synthesis using the *synth* driver in the MOOG code. We have validated line list used as follows. We first have used the linelist of the corresponding spectral region and fitted the synthesized spectrum with the solar flux atlas of Kurucz et al. (1984). Since many molecular lines are not very strong in the solar spectrum, we further repeated the procedure with the spectral atlas of Arcturus (Hinkle, et al. 2000) to corroborate the input atomic and molecular data. There are still a few unidentified features that could contribute to the uncertainties.

4.2.1. *Carbon*

The carbon abundances were derived from the C_2 Swan band lines at λ4730–4750 Å and λ5160–5167 Å. An alternate region containing CH molecules located at 4300-4310 Å (G-band) has also been used for this purpose. The C_2 lines have been shown to be useful carbon abundance indicators in carbon stars (Zamora et al. 2009) and in Galactic R Coronae Borealis stars (Hema et al. 2012). Since IRAS 16559-2957 is an O-rich star (C/O∼0.11), C

TABLE 2

SENSITIVITY OF ABUNDANCES RELATIVE TO THE UNCERTAINTIES IN THE MODEL PARAMETERS FOR IRAS 16559-2957.

Species	$\Delta\ T_{\rm eff}$ +100 K	Δ log g +0.25	$\Delta\ \xi_t$ +0.2 km s^{-1}
C	+0.02	−0.05	0.00
N	−0.05	−0.08	0.00
O I	−0.02	−0.11	+0.01
Li I	−0.12	+0.05	0.00
Na I	−0.10	0.00	+0.10
Mg I	−0.01	−0.04	+0.09
Al I	−0.07	−0.03	+0.07
Si I	+0.07	−0.12	+0.05
K I	+0.10	+0.10	+0.10
Ca I	−0.10	+0.01	+0.15
Sc II	0.00	−0.15	+0.10
Ti I	−0.17	−0.01	+0.09
V II	−0.15	−0.03	+0.17
Cr I	−0.12	+0.03	+0.13
Cr II	+0.09	−0.18	+0.05
Mn I	+0.05	+0.05	0.00
Fe I	−0.01	−0.08	+0.13
Fe II	+0.14	−0.24	+0.07
Co I	−0.01	−0.10	+0.11
Ni I	0.00	−0.10	+0.16
Cu I	+0.10	0.00	+0.20
Zn I	+0.12	−0.16	+0.05
Rb I	−0.15	0.00	0.00
Y I	−0.19	0.00	+0.07
Y II	−0.01	−0.13	+0.07
Zr I	−0.10	+0.05	0.00
Ba II	0.00	−0.10	+0.25
La II	−0.02	−0.12	+0.08
Nd II	−0.03	−0.11	+0.02
Eu II	0.00	−0.12	0.00

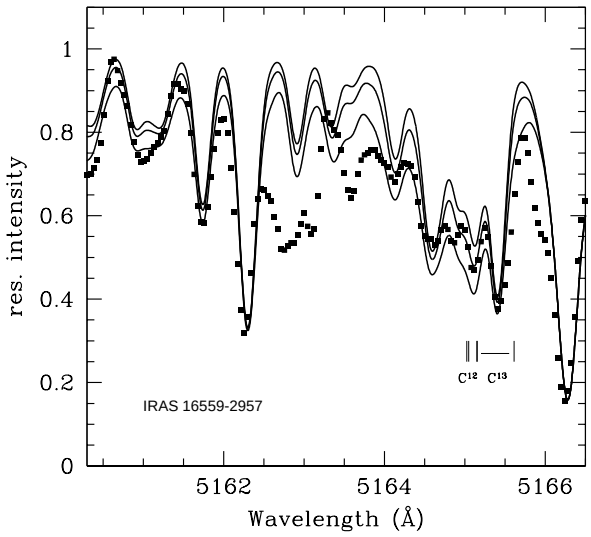

Fig. 2. Observed (filled squares) and synthetic (solid lines) spectra in the λ5165 Å C_2 band region for IRAS 16559-2957 star. The synthetic spectra correspond, from top to bottom, to log ε(C)= 7.95, 7.75, and 7.55.

being locked up in molecules is important, hence allowance was made for C in molecules CH, C2, CN and CO at the time of synthetizing C_2 and CH. For IRAS 16559-2957 the C abundance has a mean value ε(C)=7.75±0.20, i.e. the star is carbon deficient.

Figure 2 shows an example of the observed and synthetic spectra in the region around λ5165 Å .

4.2.2. *Nitrogen*

The nitrogen abundances were derived from the CN molecular lines also known as the CN red system because the molecular bands occurs at $\lambda \geq 5800$ Å. In this study we use the CN(5,1) molecular line at λ6332.18 Å. The CN(5,1) feature is affected by blends with two lines at λ6331.95 Å, one due to Si I and the other due to Fe II. Both features are taken into account in the synthesis. In order to derive the abundance of N is necessary to consider the C abundance previously obtained from Swan bands.

Figure 3 shows the observed and synthetic spectra of IRAS 16559-2957 in the region λ6331–6333 Å. We estimate a value of log ε(N)=9.2±0.3 from λ6332 Å region. This value is abnormally high and is estimated with larger uncertainty probably due to the fact that the feature is heavily blended and the region contains unidentified lines.

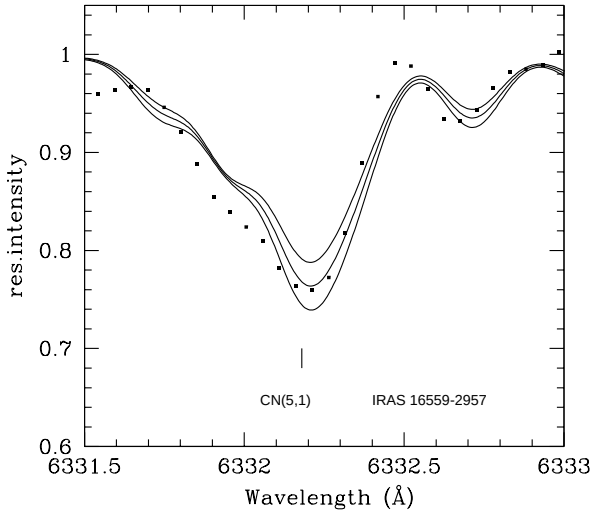

Fig. 3. Observed (filled squares) and synthetic (solid lines) spectra of the CN(5,1) band. The synthetic spectra correspond, from top to bottom to log ε(N)= 9.10, 9.20, and 9.30.

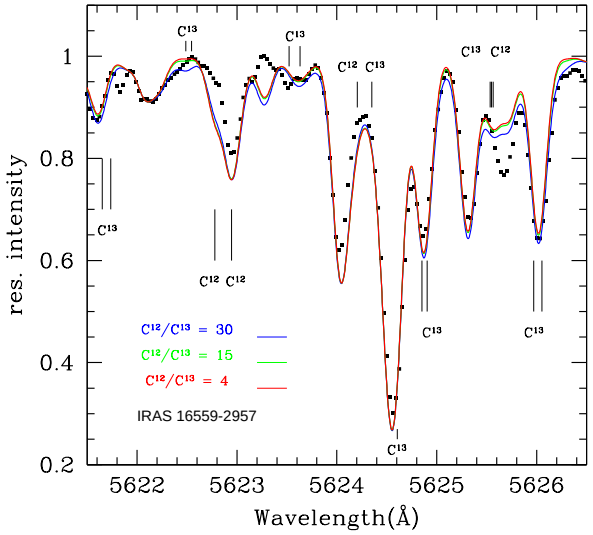

Fig. 4. Determination of ^{12}C/^{13}C isotope ratio for IRAS 16559-2957. Observed (filled squares) and synthetic (solid lines) spectra in λ5622–28 Å . Our best estimate is ^{12}C/^{13}C = 15 (green).

4.2.3. *Oxygen*

Unfortunately, the [O I] forbidden line at 6300.304 Å region is not present in the observed spectrum of IRAS 16559-2957 as it falls in an inter order gap. The [O I] line at 5577.3 gives a value ε(O)=9.0, however, it is blended with a C_2 feature and we opted for not using it. Thus, we determined the oxygen abundance from the equivalent width of the line 6363.78 Å. However, the derived value of ε(O)=8.7 should be considered an upper limit since this line seems contaminated with either nearby metallic lines or molecular CN.

4.2.4. $^{12}C/^{13}C$

The ^{12}C/^{13}C isotope ratio was determined using the features of ^{12}CN and ^{13}CN molecules in the 5622-26 Å spectral region (Fig. 4). We derived a value of the ^{12}C/^{13}C isotope ratio equal to 15.

4.2.5. *Hyper-fine structure considerations*

Hyper-fine structure (hfs) has the effect of desaturating strong lines; hence, it is important to consider hyper-fine components when performing abundance analysis of strong lines (McWilliam et al. 1995). For weak unsaturated lines the hfs treatment is not necessary.

In this analysis we have adopted the hfs data of Spite et al. (1989) and Prochaska & McWilliam (2000) for Sc II lines, Prochaska & McWilliam (2000) and Allen & Porto de Mello (2011) for Mn I lines, Mucciarelli et al. (2008) for Eu II line, McWilliam (1998) for Ba II lines, Allen & Porto de Mello (2011) for Cu I lines, Reddy et al. (2002) for Li I doublet at λ6707.7 Å and Lambert & Luck (1976) for Rb I at 7800.3 Å.

5. RESULTS AND DISCUSSION

5.1. *Derived Elemental Abundances*

In Table 4 we present the calculated elemental abundances of IRAS 16559-2957 obtained as discussed in the previous sections[4]. The solar abundances are taken from Asplund et al. (2005).

5.2. *Carbon, Nitrogen and Oxygen*

In order to infer the evolutionary status of IRAS 16559-2957 the determination of CNO abundances is required. Table 3 shows the C/O, C/N and ^{12}C/^{13}C ratios, the abundance of CNO relative to the iron abundance. An average iron abundace of [Fe/H] = +0.04±0.19 was obtained from 42 Fe I and 9 Fe II lines.

The peculiarity present in the CN abundances is the deficiency of C ([C/Fe]= −0.68) and the enhancement of N ([N/Fe]=+1.38). Our value $\sum$CNO/Fe= +0.16±0.2 is nearly solar, as expected before the

[4]We adopt the usual notation [X/H] = log $N(X)/N(H)_*$ − log $N(X)/N(H)_\odot$, wherelog $N(H) \equiv 12$ is the hydrogen abundance by number.

TABLE 3

CNO ABUNDANCES FOR IRAS 16559-2957.

C/O	C/N	$^{12}C/^{13}C$	[C/Fe]	[N/Fe]	[O/Fe]	[Fe/H]
0.11±0.08	0.04±0.03	15	−0.68±0.27	+1.38±0.42	0.00±0.19	+0.04±0.19

TABLE 4

ELEMENTAL ABUNDANCES OF IRAS 16559-2957.

Species	$\log \epsilon_\odot$	[X/H]	s.d.	N	[X/Fe]
$C(C_2)$	8.39	−0.64		syn	−0.68
N(CN)	7.78	+1.42		syn	+1.38
O I	8.66	+0.04		1	0.00
Li I	1.05	−0.07		syn	−0.11
Na I	6.17	+0.47	±0.19	3	+0.43
Mg I	7.53	+0.24	±0.16	2	+0.20
Al I	6.37	+0.10	±0.14	4	+0.06
Si I	7.51	+0.05	±0.13	8	+0.01
K I	5.08	−0.28		syn	−0.32
Ca I	6.31	+0.01	±0.09	6	−0.03
Sc II	3.05	−0.15		syn	−0.19
Ti I	4.90	−0.27	±0.12	11	−0.31
V I	4.00	+0.14	±0.15	14	+0.10
Cr I	5.64	−0.13	±0.08	2	−0.17
Cr II	5.64	−0.06	±0.13	3	−0.10
Mn I	5.39	−0.37		syn	−0.41
Fe I	7.45	+0.06	±0.13	42	
Fe II	7.45	+0.03	±0.16	9	
Co I	4.92	+0.35	±0.17	4	+0.31
Ni I	6.23	+0.28	±0.12	13	+0.24
Cu I	4.21	−0.71		syn	−0.75
Zn I	4.60	+0.08		1	+0.04
Rb I	2.60	−0.20		syn	−0.23
Y I	2.21	−0.27		1	−0.31
Y II	2.21	−0.37		1	−0.41
Zr I	2.59	−0.19		syn	−0.23
Ba II	2.17	−0.62		syn	−0.66
La II	1.13	+0.34	±0.25	2	+0.30
Nd II	1.45	−0.63		1	−0.67
Eu II	0.52	−0.22		syn	−0.26

third dredge up (Iben 1964) and being O abundance also solar, the C defficiency and its uncertainty impact on the N abundance. The uncertainty in the C abundance ±0.2 indicates that C might be underestimated by a factor of 1.6. This and the non-LTE effect may produce an overestimation of N by as much as 0.3-0.4 dex, however the N enhancement is still significant.

Strong C deficiency and N enhancement are the consquence of CN-cycled material dredged up to the suface from the He-burning shell (first dredge up) in stars upon ascending to the red giant branch. It has also been observed in core He-burning stars (Tautvaišiené et al. 2001) and in RHB stars (Afsar et al. 2012).

In massive post-AGB stars ($M > 4M_\odot$) N is also enhanced as in the hot bottom of the convective envelope carbon produced by helium burning is converted into nitrogen (Lattanzio & Wood 2004; Giridhar 2011). This keeps the C/O ratio below unity and the star does not become C-rich (Boothroyd et al. 1993). This Hot Bottom Burning process also features efficient proton capture and hence s-process element enhancements.

IRAS 16559-2957 is an O-rich (C/O ∼0.11) and is not s-process enriched. The high nitrogen abundance [N/Fe] = +1.38 clearly exceeds the mean observed values in giant ([N/Fe] = +0.35) and dwarf ([N/Fe] = +0.30) stars (Luck 1991, Reddy et al. 2006). The O abundance, [O/Fe]=0.0, is similar to those observed in giant stars ([O/Fe] ∼ +0.08) (Luck 1991; Mishenina et al. 2006; Lambert & Ries 1981; Bensby et al. 2003).

5.3. *Other heavy elements*

Other relevant abundances are addressed in this section. The Li abundance shows depletion. Theoretical predictions suggests that the stellar Li abundance, if starting from the present interstellar medium abundance log ε(Li) = 3.3, would be down to around 1.5 after the first dredge up. Hence G and K giants are expected to have low lithium abundances (Brown et al. 1989). The value found for IRAS 16559-2957, log ε(Li) = 0.98±0.13 is therefore in reasonable agreement with the first dredge-up calculations and suggests that surface Li abundance has

been depleted already during the main sequence evolution.

IRAS 16559-2957 shows relative enrichment of sodium ([Na/Fe]=+0.43). A possible source of error as explained by Mishenina et al. (2006) is non-LTE effect. Our Na abundance was calculated from three lines: 5682, 6154 and 6160 ÅÅ, with equivalent widths $\sim$ 135 mÅ for which the corrections would be in the +0.10 to +0.15 range, hence the relative enhancement of Na is real and not caused by the neglect of non-LTE treatment.

The abundances of α elements are, within the uncertainties, of solar value as they are in dwarf and giant stars of the thin disk (Reddy et al. 2003, 2006; Luck & Heiter 2007).

The abundances of iron-peak elements (Sc, V, Mn, Fe, Co, Ni) in IRAS 16559-2957 are consistent with the calculated trends by Takeda et al. (2008) and Wang et al. (2011) for field G-giants, Reddy et al. (2003; 2006) for FG-dwarfs and Reddy et al. (2012) for red giant members of open cluster.

The copper underabundance [Cu/Fe]=$-$0.75 calls our attention. This is comparable to values in metal-poor field stars (Sneden et al. 1991). Expected values for [Cu/Fe] in open cluster giants are between -0.11 to -0.23 while for normal giants of the thin disk the value is expected to be +0.01$\pm$0.13 (Reddy et al. 2012, Luck & Heiter 2007). This value defies a simple explanation.

The abundance of rubidium was obtained from spectral synthesis using the Rb I line at 7800 Å. Our synthesis profile takes into account the hyper-fine structure of the ^{85}Rb and ^{87}Rb isotopes (Lambert & Luck 1976). The fit to this line includes the Si I line at 7799.99 Å for which we took its gf value from Gustafsson et al. (2008) and we checked the atomic data of the spectral region by fitting the Arcturus spectrum (Hinkle et al. 2000). The obtained abundance value [Rb/Fe] = -0.23 ± 0.19 can be compared with the results of Carney et al. (2005) for four field giant stars in the direction of the southern warp of the Galactic disk (<[Rb/Fe]> = +0.12 $\pm$ 0.03). We find that the difference is hardly significant. Our value is also consistent with the mean abundance ratio of six giant stars in the old open clusters Be 20 and Be 29 in the outer Galactic disk (<[Rb/Fe]> = -0.09 ± 0.12) and of three giant stars in the old open cluster M67 (<[Rb/Fe]> = $-0.27 \pm$ 0.05) (Carney et al. 2005).

In the spectrum of IRAS 16559-2957 we have detected lines of the neutron capture elements Y, Zr, Ba, La, Nd, and Eu. The derived abundances of these elements are similar to those observed in field G-giants (Takeda et al. 2008; Wang et al. 2011), in FG-dwarfs (Reddy et al. 2003; 2006) and in red giant members of open cluster (Reddy et al. 2012). However we note that Ba and Nd are significantly diminished relative to those observed in dwarf and giant stars.

5.4. *Discussion*

The chemical diversity in the central stars of PAGB's is very large. They spread a large range of temperatures and masses below $8M_{\odot}$. Different families are described in detail in the thematic review by van Winckel (2003) and more recently by García-Lario (2006) and Giridhar (2011). There are two known types of O-rich PAGB's; the so called *classical*, optically bright which exhibit low metallicities ([Fe/H] between -1 and -0.3) and display a double peak in their Spectral Energy Distribution (SED), the optical one from the central star and the near-IR one from the circumstellar material. They do not display s-process enhancements and seem to be the successors of AGB stars that do not experience an efficient third dredge-up (van Winckel 2003).

The second group is formed by more massive stars ($M > 4M_{\odot}$) where the Hot Bottom Burning burns ^{12}C into ^{13}C and ^{14}N and the products are brought up to the surface via the third dredge-up; this can keep the C/O ratio below unity, mantain the ^{12}C/^{13}C ratio near the CN equilibrium value of 3.5 and dramatically enhance ^{14}N as explained by Lattanzio (2003). The stars in the later group are surrounded by dusty molecular shells responsible of IR emission and CO and OH masers.

The optical counterpart of IRAS 16559-2957 is an O-rich star, and its most prominent spectral properties found in the present paper are: mild iron defficiency [Fe/H]= $+0.04 \pm 0.19$, C/O=0.11, ^{12}C/^{13}C=15, and no signs of s-process enhancements. In fact an indicator of the influence of proton flux is the ratio of heavy to light s-process elements or [hs/ls] (Luck & Bond 1991). In IRAS 16559-2957 we calculate [hs/ls]=$-$0.04, where we have taken the abundances of Ba, La and Nd as representatives of the heavy s-process elements and Y and Zr a representative of the light ones. Typical value in s-processed enhanced PAGB's is [hs/ls]$\sim$10 (Reddy et al. 2002).

The isotope ratio ^{12}C/^{13}C is not by itself an indicator of evolution from AGB to PAGB stages and its value change dramatically between C-rich and O-rich stars. In C-rich stars a lower limit of ^{12}C/^{13}C > 20 has been found by Bakker et al. (1997) using circumstellar molecular CN red lines, and ^{12}C/^{13}C

> 25 found by Reddy et al. (2002) using ^{12}CN and ^{13}CN features in the near-IR. Values in the range 30 $<^{12}C/^{13}C<$ 70 were found in a sample of carbon stars in the Galactic disk by Lambert et al. (1986). In O-rich stars however, the first dredge up reduces the surface $^{12}C/^{13}C$ ratio and in low mass stars the inneficient third dredge up mantains the ratio low. More massive stars with an intense Hot Bottom Burning (HBB) also mantain the isotope ratio low. $^{12}C/^{13}C$ ratios as low as 3-5 has been found in O-rich planetary nebulae (Rubin et al. 2004). According to Lattanzio & Forestini (1999) low values of $^{12}C/^{13}C$ are strong evidence of HBB while high values are indication of ^{12}C dredge up without HBB and intermediate values are harder to interpret.

Thus, although not an indication of evolution in our O-rich star, our value of $^{12}C/^{13}C = 15$ is consistent with first dredge up predictions, accompanied of C decrese and N enhancement (Iben 1965). It is also comparable to the mean ratio $^{12}C/^{13}C = 16$ in the sample of mildly metal poor giants of Cottrell & Sneden (1986). Giants in older open clusters, with lower turn-off mass, exhibit values between 10 and 20 (Gilroy & Brown 1991; Smiljani et al. 2009). The clump giant stars in open clusters also shows low values of $^{12}C/^{13}C$ ratios suggesting a non-standard mixing episode occurring sometime along the upper RGB (Tautvaišiené et al. 2010).

Lithium in IRAS 16559-2957 is depleted. Lithium can be produced in AGB stars through the Cameron-Fowler Mechanism (Cameron & Fowler 1971) and large enhancements have been observed in AGB's in the Magellanic Clouds (Smith & Lambert 1990). This, which is the consequence of HBB, seems to work only in intermedite mass stars ($M > 5M_{\odot}$) (Lattanzio & Forestini 1999).

In IRAS 16559-2957 it was noted that the Na is enriched showing that the surface abundance of this element has suffered changes at the AGB, likely caused by proton capture on ^{22}Ne during the HBB phase as explained by Lattanzio (2003).

6. CONCLUSIONS

We present the results of a detailed atmospheric abundance analysis of the star IRAS 16559-2957, previously classified as a post-AGB. The analysis is based on a high resolution spectrum of the V$\sim$13 mag object at the coordinates of IRAS 16559-2957 and includes 27 elements. The photospheric chemical abundances are derived by spectral synthesis and from the equivalent widths of selected spectral lines.

Our spectrum is quite different from the low resolution spectrum published by Hu et al. (1993). The derived temperature in the present work of 4250$\pm$200K correspond more to and early K-type stars and not to an F5 as classified by these authors.

The spectral characteristcs of IRAS 16559-2957 do not correspond with the properties of O-rich PAGB's. On the other hand many of them compare with properties of giant stars at the AGB as it has been documented in §5.2 and §5.3 and §5.4.

Our results $^{12}C/^{13}C$=15 and [C/Fe]= -0.68 are consistent with first dredge up predictions (Iben 1995). We also note the presence of Rb, only observed in AGB stars, very few field giant stars and in old open clusters.

The small photospheric radial velocity of -2.3 ± 0.5 km s^{-1} ($V_{LSR} = +7.1$ km s^{-1}) is typical of the thin disk population. It is supported by near solar metallicity measured for this object. The OH maser V_{LSR} of 57–70 km s^{-1} (te Lintel Hekkert et al. 1991) correspond to the material being ejected hence red shifted to the observer. Our high resolution spectrum, and the low resolution spectrum of Hu et al. (1993) do not exhibit any emission, hence circumstellar material causing IR flux and maser may be much farther from the photosphere and cooler. OH masers in AGB stars are common (e.g. Reid et al. 1977; Bowers et al. 1989) and ocurre at distances> 10^3 AU from the central star (Reid & Moran 1981). No OH maser blue shifted component has been observed. If this scenario is correct, given the low observed stellar velocity, either the outflow is not spherically symetric or the blue component should have a velocity of ~ -60 km s^{-1}, which would indicate a very large outflow velocity, but this has been seen in some post-AGB shells, e.g. Zijlstra et al. (2001).

From the atmospheric detailed abundance analysis, we conclude that IRAS 16559-2957 is experiencing their first crossing towards the red giant branch and has probably undergone the first dredge-up. No traces of third dredge up are observed. IRAS 16559-2957 is unlikely to be a post-AGB star.

Acknowledgments

We are indebted to Prof. D.L. Lambert for permitting the use of the high resolution spectrum of IRAS 16559-2957 used in this work and to Prof. Sunetra Giridhar for her comments and suggestions on the abundance analysis. The pertinent comments and inputs of an anonymous referee are fully acknowledged. This work was supported by DGAPA-UNAM project IN104612.

REFERENCES

Afsar, M., Sneden, C., For B.Q. 2012, AJ, 144, 20

Allen, D.M., Porto de Mello, G.F. 2011, A&A, 525, 63
Alonso, A., Arribas S., Martínez-Roger, G. 1999, A&A, 140, 261
Asplund, M., Grevesse, N., Sauval, A. J. 2005, Cosmic Abundances as Records of Stellar Evolution and Nucleosynthesis in honor of David L. Lambert, ASP Conference Series, Vol. 336, p.25
Bakker, E.J., van Dishoeck, Waters, L.B.F.M., Shoenmaker, T., 1997, A&A, 323, 469
Bensby T., Feltzing S., Lundström I. 2003, A&A, 410, 527
Bonifacio, P., Caffan, E., Molaro, P., 2000, A&AS, 145, 473
Boothroyd, A.I., Sackmann, I.J., Ahern, S.C. 1993, ApJ 416, 762
Boyarchuck, A.A., Lyubimkov, L.S., Sakhibullin, N.A. 1985, Astrophysics, 22, 203
Bowers, P. F., Johnston, K. J., de Vegt, C., 1989, ApJ, 340, 479
Brown, J. A., Sneden, C., Lambert, D. L., Dutchover, E. Jr. 1989, ApJS, 71, 293
Cameron, A. G. W., Fowler, W. A. 1971, ApJ, 164, 1111
Carney, B.W., Yong, D., Teixera de Almeda, M.L., Seitzer, P. 2005, AJ, 130, 1111
Castelli F., Kurucz R.L. 2003, IAU Symposium 210, Modelling of Stellar Atmosphere, Uppsala, Sweden, eds. N.E. Piskunov, W.W. Weiss and D.F. Gray, 2003, ASP-S210
Cottrell, P. L., Sneden, C. 1986, A&A, 161, 314
Cutri, R.M., Skrutskie, M. F., van Dyk, S., et al. 2003, "2MASS All-Sky Catalog of Point Sources", in: University of Massachusetts and Infrared Processing and Analysis Center, (IPAC/California Institute of Technology) (2003)
García-Lario, P., in Planetary Nebulae in our Galaxy and Beyond, IAU Symp. 234, 2006, eds. M.J. Barlow & R.H. Méndez, p 63.
García-Lario, P., Manchado, A., Pych W., Pottasch S.R. 1997, A&AS, 126, 479
Gilroy, K.K., Brown, J.A. 1991, ApJ, 371, 578
Giridhar, S., 2011, in ASI Conferecnce Ser., eds. Pushpa Khare & C.H. Ishwara-Chadra, Vol 3, p 39
Gustafsson, B., Edvardsson, B., Eriksson, K., Jørgensen, U. G., Nordlund A. & Plez B. 2008, A&A, 486, 951
Hema, B.P., Pandey, G., Lambert D.L. 2012, ApJ, 747, 102
Hinkle K., Wallace L., Valenti, J., Harmer, D. 2000, Visible and Near Infrared Atlas of the Arcturus Spectrum 3727–9300 Å, ed. Kenneth Hinkle, Lloyd Wallace, Jeff Valenti, and Dianne Harmer, (San Francisco: ASP)
Hu, J.Y., Slijkhuis, S., de Jong, T., Jiang, B.W. 1993, A&AS, 100, 413
Kurucz, R.L., Furenlid, I., Brault, J., Testerman, L. 1984, Solar Flux Atlas from 296 to 1300 nm, National Solar Observatory, Sunspot, New Mexico.
Iben, I., 1964, ApJ, 140, 1631
Iben, I., 1965, ApJ, 142, 1447
Lambert, D.L., Luck, R. E. 1976, Obs, 96, 100
Lambert D.L., Ries L. M. 1981, ApJ, 248, 228
Lambert D.L., Gustafsson, B., Eriksson, K., Hinkle, K.H., 1986, ApJS, 62, 373
Lattanzio, J., 2003, in Planetary Nebulae: Their Evolution and Role in the Universe, eds. Sun Kwok, Michael Dopita, and Ralph Sutherland, IAU Symp. 209, 73
Lattanzio, J., Wood, P.R., 2004, in Asymptotic Giant Branch Stars, eds. Habing, H.J. & Olofsson, H., Springer-Verlag, New York Inc. p 22
Lattanzio, J., Forestini, M., 1999, in Asymptotic Giant Branch Stars, eds. T. Le Bertre, A. Lébre and C. Wealkens, IAU Symp. 192, p 31
Luck, R.E. 1991, ApJS, 75, 579
Luck, R.E., Heiter, U. 2007, AJ, 133, 2464
Luck, R. E., Bond, H.E., 1991, ApJS, 77, 515
McWilliam, A., Preston, G.W., Sneden, C., Searle, L. 1995, AJ, 109, 2757
McWilliam, A. 1998, ApJ, 115, 1640
Mishenina, T. V., Bienaymé, O., Gorbaneva, T. I., Charbonnel, C., Soubiran, C., Korotin, S. A., Kovtyukh V. V. 2006, A&A, 456, 1109
Mucciarelli, A., Caffau, E., Freytag, B., Ludwing, H.G., Bonifacio, P. 2008, A&A, 484, 841
Prochaska, J.X., McWilliam, A. 2000, AJ, 537, 57
Ramos-Larios, G., Guerrero, M.A., Suárez, O., Miranda, L.F., Gómez, J.F. 2009, A&A, 501, 1207
Reddy, A.B.S., Giridhar S., Lambert D.L. 2012, MNRAS, 419, 1350
Reddy, A.B.E., Lambert D.L., Allende Prieto A. 2006, MNRAS, 367, 1329
Reddy, A.B.E., Lambert D.L., Laws C., González G., Covey K. 2002, MNRAS, 333, 1005
Reddy, A.B.E., Tomkin, J., Lambert D.L., Allende Prieto C. 2003, MNRAS, 340, 304
Reid, M. J., Moran, J. M., 1981, ARA&A, 19, 231
Reid, M. J., Muhleman, D. O., Moran, J. M., Johnston, K. J., Schwartz, P. R., 1977, ApJ, 214, 60
Sahin, T., Lambert, D. L. 2009, MNRAS, 398, 1730
Schiller, F., Przybilla, N. 2008, A&A, 479, 849
Schlegel, D.J., Finkbeiner, D.P., Davis, M., 1998, ApJ, 500, 525
Smith, V.V., Lambert, D.L., 1990, ApJ, 361, L69
Sneden C., Gratton R.G., Crocker D.A. 1991, A&A, 246, 354
Sneden, C., 1973, PhD thesis, Univ. Texas
Spite M., Barbuy B., Spite F. 1989, A&A, 222, 35
Suárez O., García-Lario P., Manchado A., Manteiga M., Ulla A., Pottasch S.R. 2006, A&A, 458, 173
Sumangala Rao, S., Giridhar, S., Lambert, D.L., 2012, MNRAS, 419, 1254
Szczerba R., Siodimiak N., Stasinska G., Borkowski J. 2007, A&A, 469, 799
Szczerba R., Siodimiak N., Stasinska G., et al. 2012, The second release of the Toru catalogue of Galactic post-AGB objects: New classification scheme, Planetary Nebulae: An Eye to the Future, Proceedings of the International Astronomical Union, IAU Symposium,

Volume 283, p. 506-507
Takeda Y., Sato B., Murata D. 2008, PASJ, 60, 781
Tautvaišiené G., Edvardsson B., Tuominen I., Ilyin I. 2001, A&A, 380, 578
Tautvaišiené G., Edvardsson B., Puzeras E., Barisevičius G. & Ilyin I. 2010, MNRAS, 409, 1213
te Lintel Hekkert, P., Caswell, J.L., Habing, H.J., Haynes, R.F., Norris, R.P. 1991, A&AS, 90, 327
Thévenin, F., Idiart, T.P. 1999, ApJ, 521, 75
Tull, R.G., MacQueen, P.J., Sneden, C., Lambert, D.L. 1995, PASP, 107, 251
van der Veen, W.E.C.J., Habing, H.J. 1988, A&A, 194, 125
Wang, L., Liu, Y., Zhao, G., Sato, B. 2011, PASJ, 63, 1035
Zamora, O., Abia, C., Plez, B., Domínguez, I., Cristallo, S. 2009, A&A, 508, 909
Zijlstra, A.A., te Lintel Hekkert, P., Pottasch, S.R., Caswell, J.R., Ratag, M., Habing, H.J. 1989, A&A, 217, 157
Zijlstra, A. A., Chapman, J. M., te Lintel Hekkert, P., Likkel, L., Comeron, F., Norris, R. P., Molster, F. J., Cohen, R. J. 2001, MNRAS, 322, 280

R. E. Molina: Laboratorio de Investigación en Física Aplicada y Computacional, Universidad Nacional Experimental del Táchira, Venezuela, (rmolina@unet.edu.ve).
A. Arellano Ferro: Instituto de Astronomía, UNAM, Apartado Postal 70-264, 04510, México, D. F., México (armando@astro.unam.mx).